Available online at www.sciencedirect.com
ScienceDirect
Publishing Services by Elsevier
International Journal of Naval Architecture and Ocean Engineering xx (2016) 1–11
http://www.journals.elsevier.com/international-journal-of-naval-architecture-and-ocean-engineering/

# On the material properties of shell plate formed by line heating

Hyung Kyun Lim [a], Joo-Sung Lee [b,*]

[a] Hyundai Mipo Dockyard Co., Ltd., Ulsan, South Korea
[b] School of Naval Architecture and Ocean Engineering, University of Ulsan, Ulsan, South Korea

Available online ■ ■ ■

**Abstract**

This paper is concerned with investigating the plastic material properties of steel plate formed by line heating method, and is aimed at implementing more rational design considering the accidental limit states such as collision or grounding. For the present study, line heating test for marine grade steel plate has been carried out with varying plate thickness and heating speed, and then microscopic examination and tensile test have been carried out. From the microscopic, it is found that the grain refined zones like ferrite and pearlite are formed all around the heat affected zone. From the tensile test results, it is seen that yield strength, tensile strength, fracture strain, hardening exponent and strength coefficient vary with plate thickness and heat input quantity. The formulae relating the material properties and heat input parameter should be, therefore, derived for the design purpose considering the accidental impact loading. This paper ends with describing the extension of the present study.



*Keywords:* Line heating; Plasticity and fracture characteristics; Diffusion necking; Microscopic examination; Material properties; Water cooling

## 1. Introduction

Collision, grounding and stranding are major marine accidents which frequently occur in ship and offshore structures. The frequency of marine accidents of ship is increasing with the growing marine traffic and the rapid expansion of ship as a means of transportation owing to the global economic development. Among marine accidents, ship collision takes about 35% of the entire marine accidents (for example web site of KOEM). Especially in case a ship carrying detrimental liquids or oil crash, strand or explode, the leak of its pay load causes serious marine pollution. And it would cause huge environment and property loss as well as life. Along with the regulations of marine ship safety, various international conventions such as International Maritime Organization (IMO), SOLAS, MARPOL, and COLREG have been established to work hard on protecting lives, ships, and marine environment from the marine pollution. It is, however, very difficult to estimate the accurate scale of damage and fracture in case of ship collision because of the great influence of collapse behaviour, tearing pattern, and the ability to absorb collision energy following the collapse of hull structure. As it is well appreciated, for more rational ship structural design, not only the ultimate and fatigue limit states but also the accidental limit state should be properly considered at the design stage.

In real practice, when determining the arrangements and scantlings of a ship's structural members, the accidental loading due to collision is, however, not considered at the structural design stage. In addition to this, accident collision scenarios are not clearly described in the rules of the relevant classification societies, and only the extent of damage due to collisions and groundings are provided in the Harmonized Common Structural Rules, CSR-H (IACS, 2013).

Collision and grounding accidents can be categorized into the internal and the external mechanics. The external mechanics has concerned with the estimation of kinetic energy of

* Corresponding author.
*E-mail address:* jslee2@ulsan.ac.kr (J.-S. Lee).
Peer review under responsibility of Society of Naval Architects of Korea.

http://dx.doi.org/10.1016/j.ijnaoe.2016.08.001

striking and struck structures, and the internal mechanics has concerned with the dissipated energy due to plastic deformation during collision and grounding. The study on the internal mechanics of collision accident was initiated by Minorsky (1958) and many researches have been carried out in the past few decades. Amdalh (1983) conducted collision test for the bow structure by scaling down and simplifying bulbous bow structures as tubes with circular and elliptical cross-section, and proposed the simplified formulae of estimating crash strength. Numerical simulation methods have been also proposed (for example, see Wisniewski and Koiakowski, 2003). Regarding the fracture criteria, in most studies shear fracture criterion is used in dealing with the collision, contact and grounding problems. Lehmann and Yu (1998) proposed the effect of stress tri-axiality on the fracture based on the fracture mechanics of continuum, and Urban (2003) proposed RTCL model (Rice-Tracey and Cockcroft-Katham model) for the fracture criterion. The common point of these works is that fracture behaviour of material was affected by the stress tri-axiality. Recently Choung (2007) presented the plastic and fracture characteristics of marine grade steels through test and numerical studies. However, in most research, material properties obtained based on results of tensile test for the material without heat treatment have been used. The estimation of damage of striking structure as well as struck structure as accurate as possible is one of the most important tasks for a more rational design. As it is well appreciated, heat forming method usually used in manufacturing the curved blocks frequently found in bow and stern part of a ship, and much heat is inputted during heat forming process. The outer shell plates in bow or stern part of ship usually formed by cold bending process using press followed by heat forming process using line heating, triangular heating and so on. Many researches have been carried out to investigate the physical phenomena or to develop the formulae of predicting thermal deformation of line or triangular heating method (see for example Ha, 2001; Jang et al., 2001; Lee et al., 2002; Shin, 1992). Some were concerned with simulation of plate forming (Lee, 1996, 1997; Nomoto et al., 1990). Research is, however, not much concerned with the change of material properties due to heat forming which is expected to much affect the shape and extents of structural damage subjected to the impact loading due to collision, grounding and so on. In order to predict the extent and shape of damage as accurate as possible, it is, therefore, necessary to investigate the change in material properties due to heat forming of structural part which may be a part of striking structure or struck structure when collision accident occurs.

The paper is aimed at investigating the material characteristics of shell plate formed by line heating far beyond the elastic region in order to implement reasonable design considering the accidental limit states such as collision or stranding. Line heating test for the marine grade steel is carried out with varying the heating speed and plate thickness and with keeping the same heat input condition. Water cooling method is applied as a cooling method to simulate the real practice in plate forming process in real shipyard. Microscopic examination is conducted by taking specimens after line heating test to observe changes in micro-structure at the heat affect zone due to heating. A series of tensile test are conducted in order to get the material properties of marine grade steel far beyond the elastic region when the line heating is applied. The material properties, that is, yield strength, tensile strength, fracture strain, hardening exponent and strength coefficient are extracted based on the results of tensile tests. And through the statistical analysis of above data, plastic strain hardening exponent and strength coefficient are provided, which are basic parameters in Hollomon's constitutive equation.

## 2. Plastic hardening constitutive equation

Tensile test of steel plate is usually conducted to get the elasto-plastic material properties such as elastic modulus, yield strength, tensile strength, strain hardening exponent, and strength coefficient. Fig. 1 illustrates the typical example of stress-strain curve that can be derived through tensile test. The plastic material property considerably affects the result of the structural analysis when fracture and large strain are accompanied under the accidental load due to collision of ships. The relation between elongation and load can be, however, can be applied until the diffusion necking occurs intensively around some cross-section of member, which is called uniform true stress-uniform true strain.

Nominal strain in a uniaxial tensile test is expressed as Eq. (1).

$$\varepsilon = \frac{\Delta L}{L_0} = \frac{L - L_0}{L_0} \tag{1}$$

Nominal stress is expressed in terms of uniaxial load P as Eq. (2).

$$S = \frac{P}{A_0} \tag{2}$$

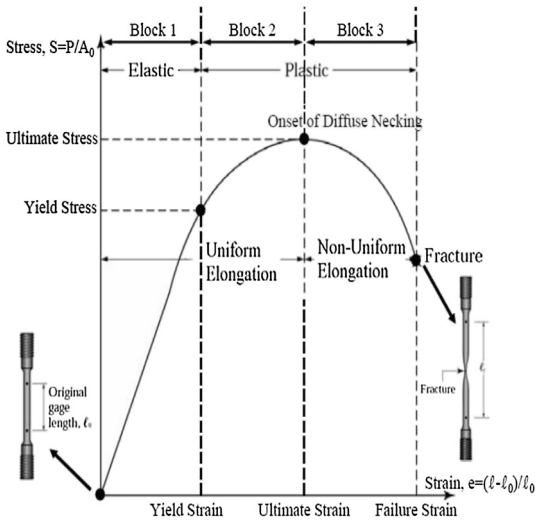


Fig. 1. Engineering stress-strain representing typical three blocks in ductile metal specimen under tensile load (Kalpakjian and Schmid, 2001).

Please cite this article in press as: Lim, H.K., Lee, J.-S., On the material properties of shell plate formed by line heating, International Journal of Naval Architecture and Ocean Engineering (2016), http://dx.doi.org/10.1016/j.ijnaoe.2016.08.001

The uniform true stress and the uniform true strain at deformed section before the diffusion necking occurs as follows.

$$\sigma = \frac{P}{A} = S(1+\varepsilon) \tag{3}$$

Plastic deformation rate corresponding to the gauge length at a particular section is defined as in Eq. (4), which is called the log true strain that can be applied before the diffusion necking.

$$\varepsilon^p = \int_{L_0}^{L} d\varepsilon^p = \int_{L_0}^{L} \frac{dL}{L} = ln\frac{L}{L_0} = \ln(e+1) \tag{4}$$

where $L_0$ is initial gauge length, and L is the gauge length at a particular section. Hollomon showed the stress-strain relation in plastic range with using hardening exponent, $n$ and strength coefficient, $K$ as in Eq. (5). In this expression, the strain hardening exponent, $n$ denotes the gradient of stress-strain curve.

$$\sigma = K(\varepsilon^p)^n \tag{5}$$

According to ASTM E646-07, the strain hardening exponent, $n$ and the strength coefficient, $K$ are defined as follows.

$$n = \frac{N\sum_{i=1}^{N} x_i y_i - \sum_{i=1}^{N} x_i \sum_{i=1}^{N} y_i}{N\sum_{i=1}^{N} x_i^2 - \left(\sum_{i=1}^{N} x_i\right)^2} \tag{6}$$

$$K = exp\left[\frac{\sum_{i=1}^{N} y_i - n\sum_{i=1}^{N} x_i}{N}\right] \tag{7}$$

where $x = log\sigma$, $y = log\varepsilon$ and $N$ is number of data.

Table 1
Condition of line heating test.

| Item | Value or description |
|---|---|
| Heat source | LPG |
| LPG pressure | 1.7 kgf/cm$^2$ |
| Oxygen pressure | 4 kgf/cm$^2$ |
| LPG flow rate | 23 L/min |
| Oxygen flow rate | 50 L/min |
| Distance between torch tip and plate surface | 50 mm |
| Torch tip number | 3000 |
| Cooling method | Water cooling |

## 3. Line heating experiment

Line heating test has been carried out to investigate the effect of heat input on material properties such as yield strength, tensile strength and so on. The test specimens were made of marine A-grade mild steel of which nominal yield strength is 235 MPa and which is frequently used as shell plates. For the round specimen only, Bridgman's necking correction formula (1952) is generally used to revise triaxial stress state of tensile specimen after necking. But in case of flat specimen, Bridgmans' formula cannot be used because of the invalidity of axial symmetry hypothesis. In this study, in order to investigate plastic material characteristics of marine grade steel plate with heat forming by line heating for a more rational design of ship structure, numerical analysis for the thermal elasto-plastic behaviour and tensile test is conducted with varying heat input and the thickness with using the elasto-plastic properties of marine grade steel derived for the steel specimen on which heat treatment is applied by line heating. Before line heat test, the initial displacements along the heating direction are measured. After heating and cooling processes, displacements are measured at the same locations to derive the deformation due to line heating. For the present test, the displacements were measured with laser sensor whose resolution was ±0.2 mm. Four K-type thermocouples were attached on the back side of heating to measure temperature at locations 0, 10, 20, 50 mm apart from the centre of heating line, respectively.

The most dominant parameter affecting the result of linear heating is the heat input. The heat input per the unit time of the present line heating apparatus is 23 122.8 J/sec. The size of specimen is 300*1000 mm. The line heating test was conducted with varying heating speed as 400, 500 and 600 mm/min for 10 mm and 15 mm thick specimen to investigate the change in material properties to thickness of plate as well as heat input. Water cooling was applied at the location 150 mm apart from the heating torch to trigger phase transition due to line heating. Conditions for the present line heating test are summarized in Table 1. Fig. 2 illustrates the present line heating test scene.

The temperature histories at the back side of heated surface during test are illustrated in Fig. 3 for 10 mm thick specimen when heating speed is 400, 500 and 600 mm/min, respectively. As it can be easily expected, the peak temperature becomes

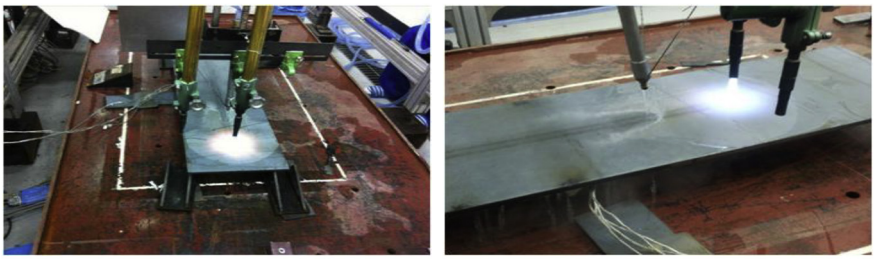

a) Line heating apparatus b) Water cooling during line heating

Fig. 2. Present line heating apparatus and line heating experiment.

Please cite this article in press as: Lim, H.K., Lee, J.-S., On the material properties of shell plate formed by line heating, International Journal of Naval Architecture and Ocean Engineering (2016), http://dx.doi.org/10.1016/j.ijnaoe.2016.08.001

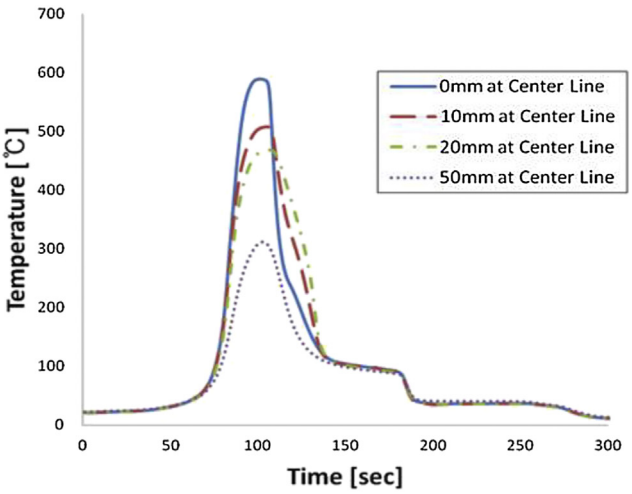


(a) Heating speed : 400mm/sec

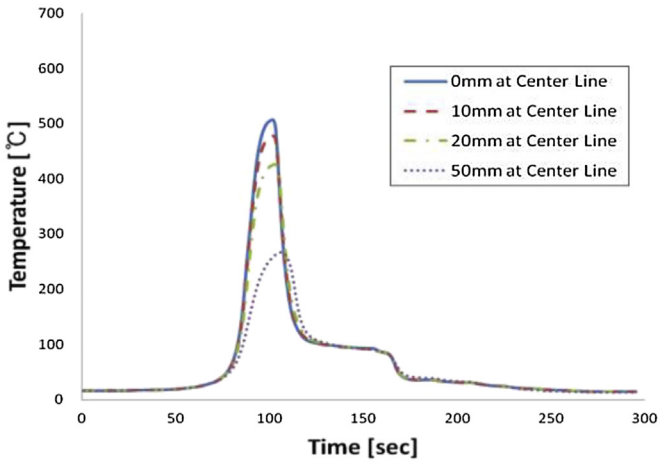


(b) Heating speed : 500mm/sec

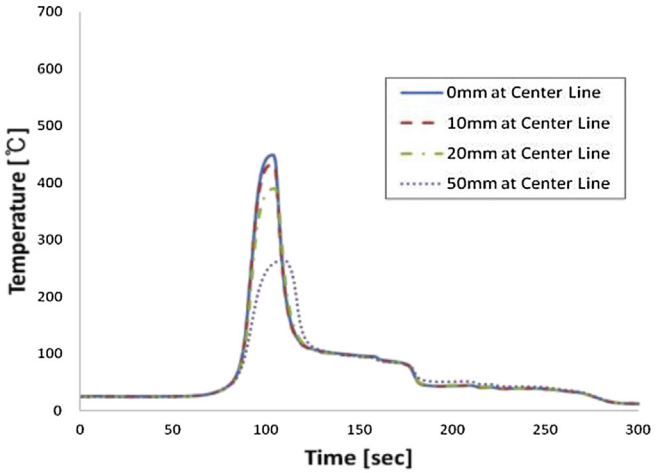


(c) Heating speed : 600mm/sec

Fig. 3. Temperature history of 10 mm steel.

higher as heating speed becomes slower due to higher heat input during line heating, and temperature suddenly decreases just after water cooling.

### 3.1. Microscopic examination

In order to observe the micro-structure of line heated section, microscopic examination was conducted after cutting the mid-section of specimen with wire cutting machine. Cut section was polished through due process (see Fig. 4). Fig. 5 shows microscopic scanning position of the polished cut section.

The width and depth of heat affect zone can be calculated by using the equations proposed by Satoh and Terasaki (1976). The equation for width, $w$ was given as

$$w = 9.67\sqrt{\frac{Q}{v(T_{\max} - T)_i}} \tag{8}$$

where Q is heat input per unit time in cal/sec and v is heating speed in cm/sec. $T_{max}$ and $T_i$ are $Ac_3$ temperature of steel and room temperature, respectively. That is, Ac3 is the temperature that austenite transformation is completed and is the parameter associated with the width of heat affect zone and determined as following Eq. (9)

$$A_{C_3} = 910 - 203\sqrt{C} - 15.1Ni + 44.7Si + 104V + 31.5Mo + 13.1W \tag{9}$$

$Ac_3$ temperature of steel is calculated from Eq. (9) and the width of heat affected zone is estimated based on the temperature distribution by the thermo-elasto-plastic analysis. The depth of heat affect zone, $d$ was given as

$$d = \frac{1}{4200}\frac{Q}{vt} \tag{10}$$

where $t$ is thickness of steel plate. Some results of width and depth of heat affect zone (HAZ) are illustrated in Table 2. $w$ and $d$ normalized by plate thickness are plotted against the heat input, $Q/vt$ as in Fig. 6. As it can be easily expected, both $w/t$ and $d/t$ increase as heat input parameter increases.

Fig. 7 is the photo magnified by 1000 times with an optical microscope to show the surface of heat affected zone along the depth. As it is seen in Fig. 7, through the phase transition resulted from line heating, the grain refined zones like ferrite(white) and pearlite(black) are formed around the whole heat affected zone. However, the martensite transformation reported in many references was not found. It is because ferrite phase exists as fine grains which are not able to be transformed into austenite phase and grow due to relatively low peak temperature. In other words, fine precipitates that restrain grain growth cannot dissolve or coarsen, and so only fine ferrite and pearlite phases exist without grain growth after the phase transition from austenite to ferrite during cooling process.

Please cite this article in press as: Lim, H.K., Lee, J.-S., On the material properties of shell plate formed by line heating, International Journal of Naval Architecture and Ocean Engineering (2016), http://dx.doi.org/10.1016/j.ijnaoe.2016.08.001

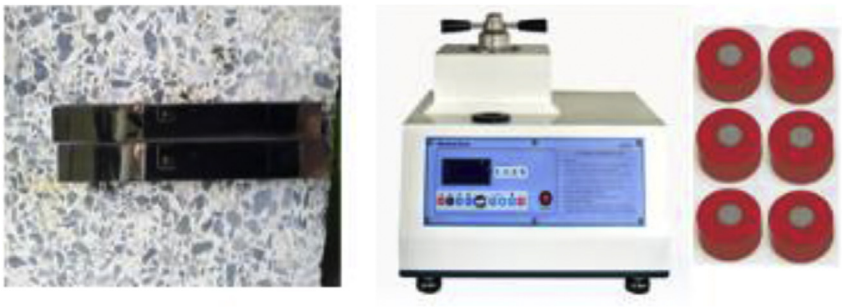

(a) Polishing (b) Mounting

Fig. 4. Polishing and mounting for microscopic examination.

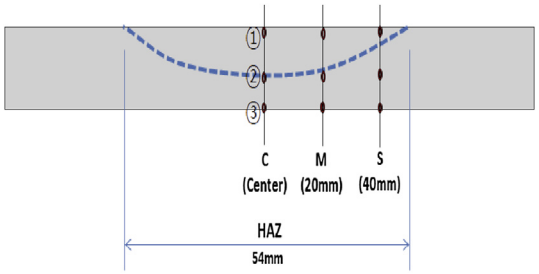


Fig. 5. Scanning positions of optical microscope in HAZ by line heating.

## 4. Tensile test

### 4.1. Shape and dimension of specimen

Specimens for tensile test were taken to investigate the physical properties of the plastically deformed material due to the line heating experiment described in the previous section. In order to minimize the additional heat input into specimen while taking specimen by cutting method, wire cutting machine was used, which was known as one of the best way to minimize the generated heat effect comparing with plasma or normal oxygen cutting. Tensile specimen is made according to standards described in ASTM (2004) and also JIS (1998). Dimensions of specimen for tensile test are shown in Fig. 8, in which dotted area in the middle of tensile coupon just denotes the region within gauge length. Although steel plate is known to be nearly close to isotropic material, line heating test were conducted in the direction parallel to the roll direction and also normal to the roll direction to show the discrepancy to roll direction, and specimens for tensile test were taken along the heating direction. Table 3 shows the data for specimens, in which plate thickness, heating speed and heating direction are included. In the same table 'Parallel' and 'Normal' denote the heating direction parallel and normal to roll direction of steel plate, respectively, and '(non-heating)' denotes the specimens which were taken from raw steel plate without heating forming. For all cases, three specimens were taken, and so the total number of specimens is 48.

Table 2
Width and depth of heat affect zone due to line heating estimated based on the numerical analysis result.

| Serial no. | Thickness (mm) | Heating speed (mm/min) | Heat input per time (cal/sec) | Width of HAZ, $w$ (mm) | Depth of HAZ, $d$ (mm) |
|---|---|---|---|---|---|
| 1 | 10.0 | 300 | 2300 | 47.0 | 10.0 |
| 2 | 10.0 | 400 | 2300 | 31.0 | 4.4 |
| 3 | 10.0 | 500 | 2300 | 22.0 | 1.7 |
| 4 | 12.5 | 300 | 2300 | 41.2 | 7.3 |
| 5 | 12.5 | 400 | 2300 | 20.0 | 1.8 |
| 6 | 15.0 | 300 | 2300 | 33.0 | 4.5 |

### 4.2. Tensile test

Tensile test was conducted for 48 specimens shown in Table 2 using 300 kN universal tensile test apparatus shown in Fig. 9. Test speed was 2.0 mm/min. Elongation was measured with the extensometer whose gauge length was 50 mm.

Fig. 10 shows the typical example of fracture surface of the heated specimen by line heating method. Flat fracture surface mainly occurred in central fracture surface because of tensile stress, and slant fracture surface occurred in surroundings because of shear stress.

Diffusion necking and fractures which occur during the tensile test are shown in Fig. 11. The main purpose of this

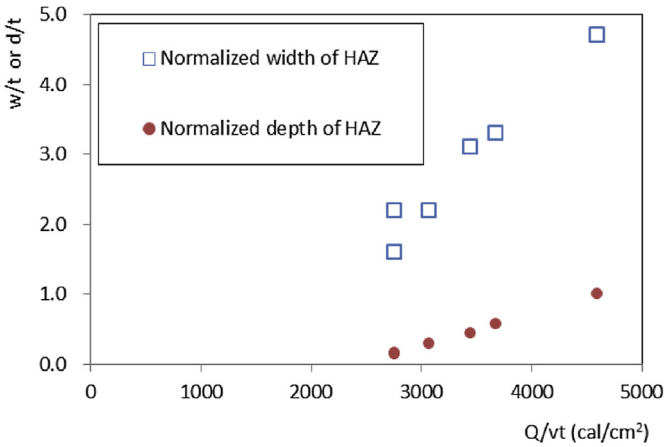


Fig. 6. Width and depth of HAZ against heat input for the present study.

Please cite this article in press as: Lim, H.K., Lee, J.-S., On the material properties of shell plate formed by line heating, International Journal of Naval Architecture and Ocean Engineering (2016), http://dx.doi.org/10.1016/j.ijnaoe.2016.08.001

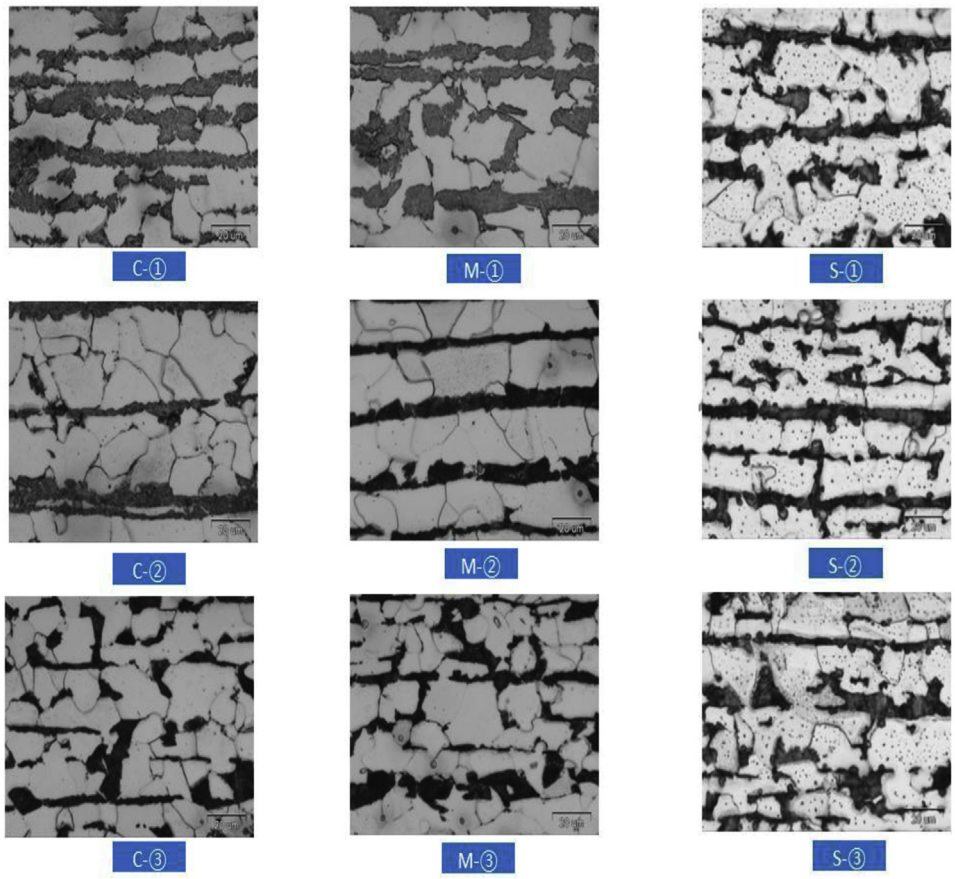


a) 0mm from heating line b) 20mm from heating line c) 40mm from heating line

Fig. 7. Scanning optical microscopic examination magnified by 1000 times (heating speed: 400 mm/min).

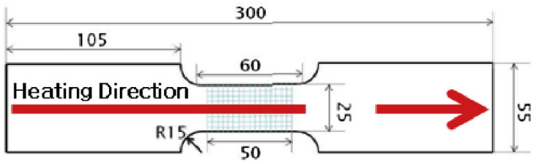


Fig. 8. Dimensions of specimen for tensile test (mm).

study is to obtain material properties of heat formed steel plate by line heating method, and so material properties such as yield strength, $\sigma_y$, tensile strength, $\sigma_U$, fracture strain, $\varepsilon_f^P$, hardening exponent, $n$ and strength coefficient, $K$ are derived based on the results of tensile tests for 48 specimens in Table

Table 3
Prepared specimens for tensile test [mm].

| Serial | Thickness(mm) | Heating speed (mm/min) | Heating direction | Quantity |
|---|---|---|---|---|
| F1 | 10.0 | (non-heating) | Parallel | 3 |
| F2 | 10.0 | (non-heating) | Normal | 3 |
| F3 | 10.0 | 400 | Parallel | 3 |
| F4 | 10.0 | 400 | Normal | 3 |
| F5 | 10.0 | 500 | Parallel | 3 |
| F6 | 10.0 | 500 | Normal | 3 |
| F7 | 10.0 | 600 | Parallel | 3 |
| F8 | 10.0 | 600 | Normal | 3 |
| F9 | 15.0 | (non-heating) | Parallel | 3 |
| F10 | 15.0 | (non-heating) | Normal | 3 |
| F11 | 15.0 | 400 | Parallel | 3 |
| F12 | 15.0 | 400 | Normal | 3 |
| F13 | 15.0 | 500 | Parallel | 3 |
| F14 | 15.0 | 500 | Normal | 3 |
| F15 | 15.0 | 600 | Parallel | 3 |
| F16 | 15.0 | 600 | Normal | 3 |


Fig. 9. 300 kN tensile test apparatus.

Please cite this article in press as: Lim, H.K., Lee, J.-S., On the material properties of shell plate formed by line heating, International Journal of Naval Architecture and Ocean Engineering (2016), http://dx.doi.org/10.1016/j.ijnaoe.2016.08.001

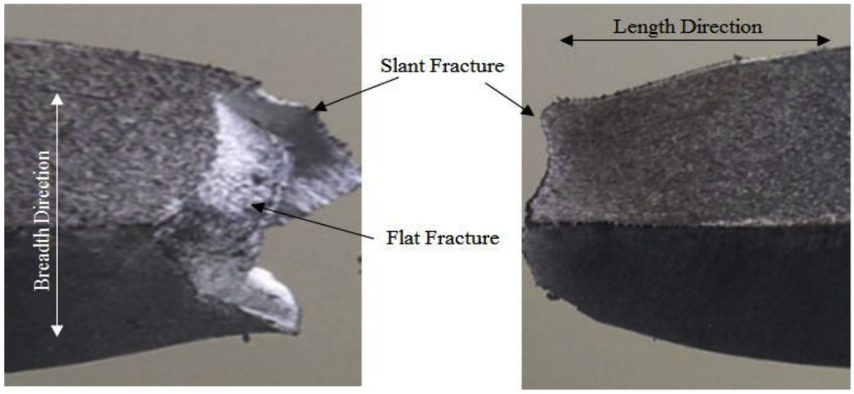


Fig. 10. Fractured plane of a flat specimen.

3. Tensile test results of 48 specimens are listed in Table 4 for 10 mm thick specimens and in Table 5 for 15 mm thick specimens. In Table 6 results are summarized according to heating speed, that is, non-heating, heating speed of 600, 500 and 400 mm/min, respectively. The first three are results of specimens taken in the parallel direction to rolling direction and the last three those taken in the normal direction to rolling direction. There is difference in mechanical properties according to the direction of specimen taken, but not much great. In the same tables, S.D and COV denote 'standard deviation' and 'coefficient of variation' of 6 specimens of each case. Mean and COV of 5 material properties are summarized in Table 4. As it can be seen, for all cases of specimens COV of material properties is less than 0.05, that is, 5% except those of hardening exponent, $n$ and strength coefficient, $K$ for the case of heating speed, $v$ of 400 mm/min (see also Table 4(d) and 4(d)).

Average nominal stress-strain curves derived from the tensile test are represented in Figs. 12 and 13 for 10 and 15 mm thick specimens, respectively. And with the true stress-strain data extracted from Eq. (5), the average true stress-strain curves are shown in Fig. 14. From the tensile test results shown in Tables 4 and 5, and Figs. 12–14, yield strength, tensile strength and strength coefficient, $K$ increase as heating

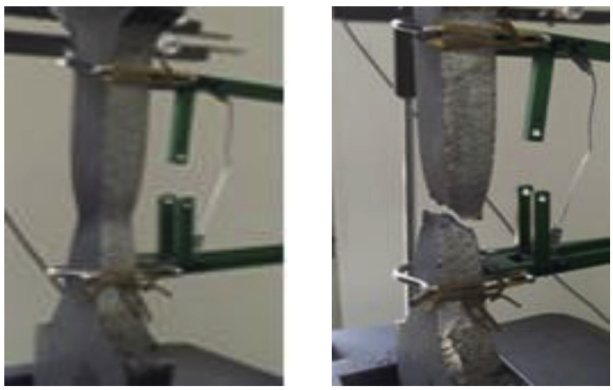

(a) After diffuse necking (b) After Fracture

Fig. 11. Necking and fracture of specimen.

Table 4
Derived mechanical properties: $t = 10$ mm.

| Serial no | $\sigma_y$ (MPa) | $\sigma_U$ (MPa) | $\varepsilon_f^P$ | $n$ | $K$ (MPa) |
|---|---|---|---|---|---|
| **(a) non-heating** | | | | | |
| F1-1 | 304.06 | 455.72 | 1.301 | 0.170 | 907.6 |
| F1-2 | 317.34 | 469.47 | 1.289 | 0.168 | 890.2 |
| F1-3 | 300.97 | 451.87 | 1.319 | 0.163 | 852.4 |
| F2-1 | 303.92 | 451.86 | 1.312 | 0.165 | 874.7 |
| F2-2 | 299.45 | 448.21 | 1.341 | 0.167 | 886.8 |
| F2-3 | 296.37 | 447.01 | 1.359 | 0.169 | 912.6 |
| Mean | 303.69 | 454.02 | 1.320 | 0.167 | 887.4 |
| S.D | 7.28 | 8.17 | 0.026 | 0.003 | 22.1 |
| COV | 0.024 | 0.018 | 0.020 | 0.016 | 0.025 |
| **(b) $v$ = 600 mm/min** | | | | | |
| F7-1 | 351.96 | 480.84 | 1.280 | 0.173 | 984.5 |
| F7-2 | 352.21 | 480.93 | 1.300 | 0.174 | 981.3 |
| F7-3 | 337.16 | 472.26 | 1.326 | 0.168 | 936.7 |
| F8-1 | 358.65 | 480.73 | 1.301 | 0.177 | 997.5 |
| F8-2 | 346.84 | 476.35 | 1.339 | 0.169 | 1010.6 |
| F8-3 | 341.78 | 474.48 | 1.341 | 0.175 | 992.8 |
| Mean | 348.10 | 477.60 | 1.315 | 0.173 | 983.9 |
| S.D | 7.80 | 3.77 | 0.025 | 0.004 | 25.3 |
| COV | 0.022 | 0.008 | 0.019 | 0.020 | 0.026 |
| **(c) $v$ = 500 mm/min** | | | | | |
| F5-1 | 369.41 | 485.20 | 1.270 | 0.173 | 1022.6 |
| F5-2 | 357.94 | 483.17 | 1.293 | 0.176 | 1031.3 |
| F5-3 | 346.11 | 487.20 | 1.252 | 0.192 | 1109.2 |
| F6-1 | 376.89 | 490.08 | 1.281 | 0.179 | 1021.6 |
| F6-2 | 351.16 | 473.72 | 1.314 | 0.186 | 1043.3 |
| F6-3 | 350.49 | 479.21 | 1.303 | 0.193 | 1066.3 |
| Mean | 358.67 | 483.10 | 1.286 | 0.183 | 1049.1 |
| S.D | 12.08 | 5.88 | 0.023 | 0.008 | 33.8 |
| COV | 0.034 | 0.012 | 0.002 | 0.005 | 0.032 |
| **(d) $v$ = 400 mm/min** | | | | | |
| F3-1 | 384.90 | 498.24 | 1.263 | 0.193 | 1217.6 |
| F3-2 | 386.63 | 500.48 | 1.246 | 0.179 | 1028.6 |
| F3-3 | 370.20 | 472.18 | 1.271 | 0.216 | 1114.0 |
| F4-1 | 380.76 | 495.76 | 1.277 | 0.182 | 1136.6 |
| F4-2 | 386.48 | 499.54 | 1.268 | 0.220 | 1291.8 |
| F4-3 | 374.97 | 487.43 | 1.279 | 0.208 | 1134.2 |
| Mean | 380.66 | 492.27 | 1.267 | 0.200 | 1153.8 |
| S.D | 6.77 | 10.91 | 0.012 | 0.018 | 90.6 |
| COV | 0.018 | 0.022 | 0.009 | 0.088 | 0.079 |

[Note] S.D: standard deviation, COV: coefficient of variation.

Please cite this article in press as: Lim, H.K., Lee, J.-S., On the material properties of shell plate formed by line heating, International Journal of Naval Architecture and Ocean Engineering (2016), http://dx.doi.org/10.1016/j.ijnaoe.2016.08.001

Table 5
Derived mechanical properties: $t = 15$ mm.

| Serial no | $\sigma_y$(MPa) | $\sigma_U$(MPa) | $\varepsilon_f^P$ | $n$ | $K$ (MPa) |
|---|---|---|---|---|---|
| **(a) non-heating** | | | | | |
| F9-1 | 284.93 | 449.45 | 1.376 | 0.163 | 885.1 |
| F9-2 | 279.11 | 440.13 | 1.380 | 0.167 | 899.5 |
| F9-3 | 291.55 | 455.38 | 1.352 | 0.176 | 964.9 |
| F10-1 | 281.49 | 452.62 | 1.356 | 0.169 | 926.0 |
| F10-2 | 277.03 | 444.38 | 1.341 | 0.161 | 872.4 |
| F10-3 | 279.07 | 446.36 | 1.325 | 0.171 | 881.5 |
| Mean | 282.20 | 448.05 | 1.355 | 0.168 | 904.9 |
| S.D | 5.32 | 5.58 | 0.021 | 0.005 | 34.9 |
| COV | 0.019 | 0.012 | 0.015 | 0.033 | 0.039 |
| **(b) $v = 600$ mm/min** | | | | | |
| F15-1 | 303.27 | 468.94 | 1.369 | 0.175 | 948.4 |
| F15-2 | 309.16 | 471.05 | 1.355 | 0.177 | 956.7 |
| F15-3 | 305.62 | 467.95 | 1.363 | 0.172 | 942.5 |
| F16-1 | 303.46 | 468.41 | 1.330 | 0.181 | 971.0 |
| F16-2 | 306.99 | 469.78 | 1.315 | 0.182 | 969.2 |
| F16-3 | 301.16 | 468.52 | 1.324 | 0.196 | 1075.4 |
| Mean | 304.94 | 469.11 | 1.343 | 0.181 | 977.2 |
| S.D | 2.89 | 1.13 | 0.023 | 0.008 | 48.4 |
| COV | 0.009 | 0.002 | 0.017 | 0.047 | 0.051 |
| **(c) $v = 500$ mm/min** | | | | | |
| F13-1 | 325.46 | 471.40 | 1.345 | 0.182 | 1053.9 |
| F13-2 | 313.57 | 469.91 | 1.359 | 0.194 | 1114.0 |
| F13-3 | 316.37 | 475.78 | 1.316 | 0.180 | 1097.2 |
| F14-1 | 312.19 | 469.45 | 1.314 | 0.175 | 1059.9 |
| F14-2 | 305.61 | 476.04 | 1.287 | 0.176 | 1073.7 |
| F14-3 | 309.16 | 464.36 | 1.321 | 0.200 | 1170.0 |
| Mean | 313.73 | 471.16 | 1.324 | 0.185 | 1094.8 |
| S.D | 6.84 | 4.38 | 0.025 | 0.010 | 43.3 |
| COV | 0.022 | 0.009 | 0.019 | 0.055 | 0.040 |
| **(d) $v = 400$ mm/min** | | | | | |
| F11-1 | 327.76 | 477.68 | 1.290 | 0.211 | 1259.2 |
| F11-2 | 325.76 | 473.83 | 1.358 | 0.195 | 1163.3 |
| F11-3 | 310.17 | 477.08 | 1.324 | 0.189 | 1121.5 |
| F12-1 | 323.02 | 474.40 | 1.299 | 0.194 | 1147.4 |
| F12-2 | 320.06 | 472.67 | 1.314 | 0.181 | 1073.2 |
| F12-3 | 315.54 | 471.35 | 1.287 | 0.232 | 1274.7 |
| Mean | 320.39 | 474.50 | 1.312 | 0.200 | 1173.2 |
| S.D | 6.61 | 2.47 | 0.027 | 0.018 | 78.9 |
| COV | 0.021 | 0.005 | 0.020 | 0.092 | 0.067 |

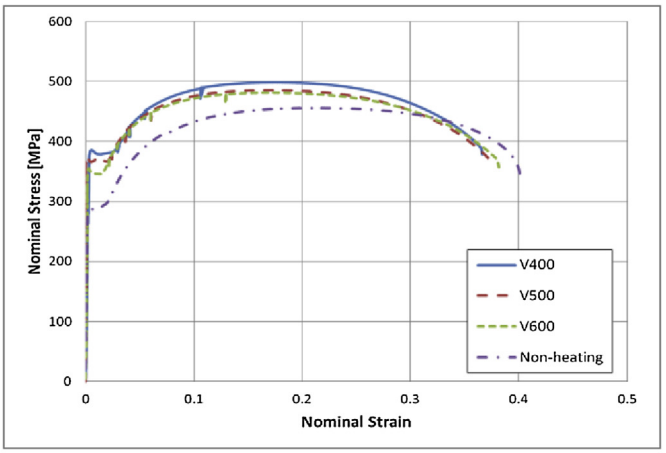


(a) Heating parallel to rolling direction

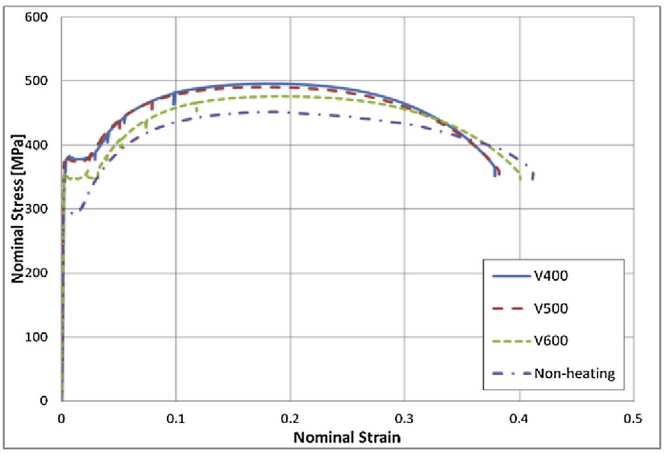


(b) Heating normal to rolling direction

Fig. 12. Average nominal stress-strain curves of 10 mm thick specimens.

speed decreases, that is, as heat input increases, while fracture strain, $\varepsilon_f^P$ and hardening exponent, $n$ generally decrease. As it can be seen in Figs. 12 and 13, the yield strength and tensile strength of heated steel plate have increased by about 15–25% and 4–9%, respectively comparing with those of unheated plate. The fracture strain, however, has been reduced by about

Table 6
Mean and COV of material properties for the present specimens in Table 3.

| Serial no | Heating speed (mm/min) | $\sigma_y$ (MPa) | $\sigma_U$ (MPa) | $\varepsilon_f^P$ | $n$ | $K$ (MPa) |
|---|---|---|---|---|---|---|
| **(a) $t = 10.0$ mm** | | | | | | |
| F1, F2 | (non-heating) | 303.69 (0.024) | 454.02 (0.018) | 1.320 (0.020) | 0.167 (0.016) | 887.4 (0.025) |
| F7, F8 | 600 | 348.10 (0.022) | 477.60 (0.008) | 1.315 (0.019) | 0.173 (0.020) | 983.9 (0.026) |
| F5, F6 | 500 | 358.67 (0.034) | 483.10 (0.012) | 1.286 (0.002) | 0.183 (0.005) | 1049.1 (0.032) |
| F3, F4 | 400 | 380.66 (0.018) | 492.27 (0.022) | 1.267 (0.009) | 0.200 (0.088) | 1153.8 (0.079) |
| **(b) $t = 15.0$ mm** | | | | | | |
| F9, F10 | (non-heating) | 282.20 (0.019) | 448.05 (0.012) | 1.355 (0.015) | 0.168 (0.033) | 904.9 (0.039) |
| F15, F16 | 600 | 304.94 (0.009) | 469.11 (0.002) | 1.343 (0.017) | 0.181 (0.047) | 977.2 (0.051) |
| F13, F14 | 500 | 313.73 (0.022) | 471.16 (0.009) | 1.324 (0.019) | 0.185 (0.055) | 1094.8 (0.040) |
| F11, F12 | 400 | 320.39 (0.021) | 474.50 (0.005) | 1.312 (0.020) | 0.200 (0.092) | 1173.2 (0.067) |

[Note] Figure in parenthesis is COV (coefficient of variation).

Please cite this article in press as: Lim, H.K., Lee, J.-S., On the material properties of shell plate formed by line heating, International Journal of Naval Architecture and Ocean Engineering (2016), http://dx.doi.org/10.1016/j.ijnaoe.2016.08.001

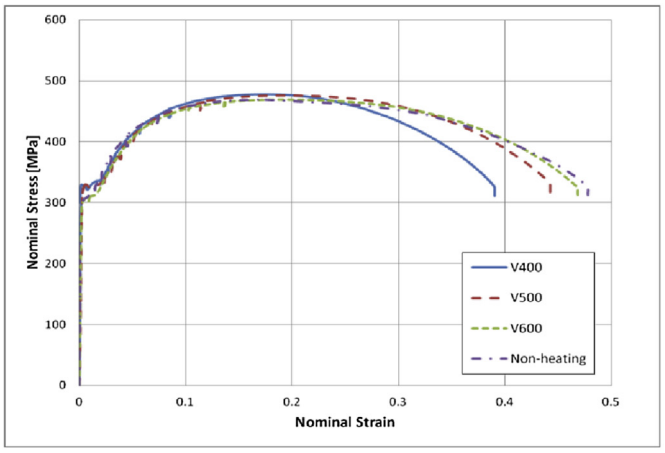


(a) Heating parallel to rolling direction

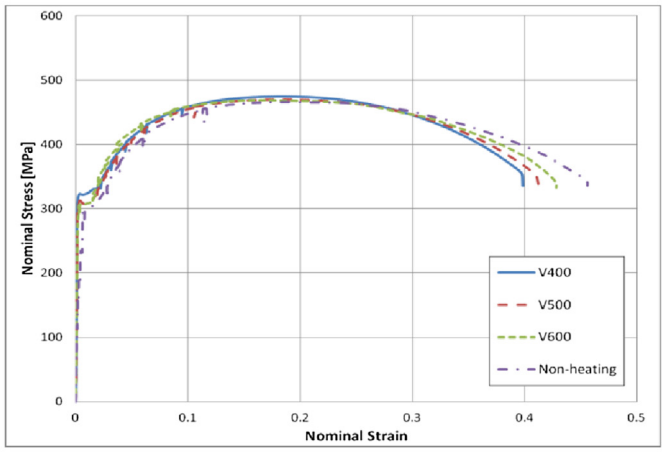


(b) Heating normal to rolling direction

Fig. 13. Average nominal stress-strain curves of 15 mm thick specimens.

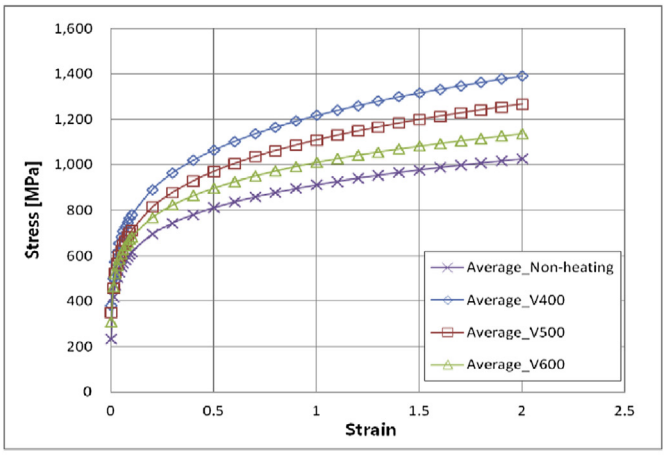


(a) $t$= 10mm

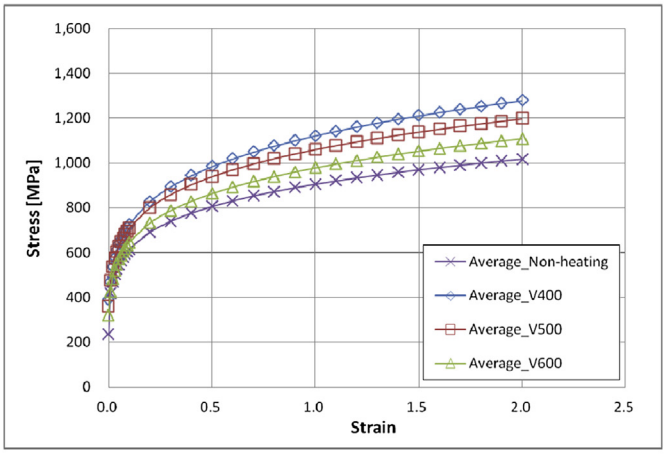


(b) $t$ = 15mm

Fig. 14. Average true stress-strain curves.

3–5%. From these findings energy absorbed till rupture by the heated plate usually less than that of unheated plate. It can be also found that the five material properties seem to depend upon both heat input and plate thickness. The relations between five material properties such as yield strength, tensile strength and so on and heat input parameter, $q$ which is defined as Eq. (11) are plotted as in Figs. 14–19 for each material property to illustrate their dependency upon heat input.

$$q = \frac{Q_{eff}}{t\sqrt{vt}} \tag{11}$$

In Eq. (11) $Q_{eff}$ is the effective heat power and is 23 122.8 J/sec for the present heating apparatus shown in Fig. 3 with heating conditions in Table 1. There are several definitions for the heat input parameter (for example see Masubuchi (1980)). Among them Eq. (11) can reflect effects of plate thickness as well as heat input.

As far as the present test results are concerned, the important material properties such as yield strength and so on significantly varies with heat input. This should be, therefore, reflected in the design of structural members which are manufactured with heat treatment such as the curved surface found at bow or stern of a ship surface, especially when the design is principally governed by the impact. Since the number of data shown in Figs. 15–19 is too small to be used in deriving relationships between each material property and heat

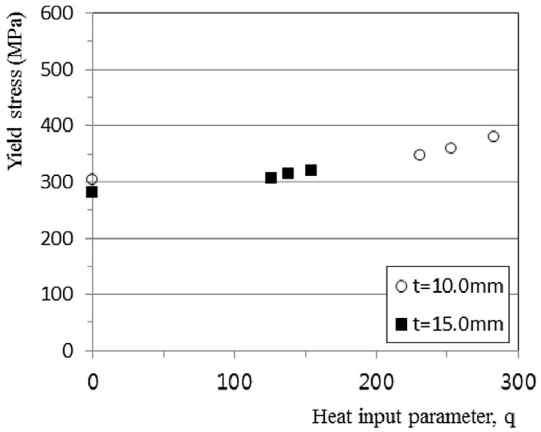


Fig. 15. Yield strength vs heat input parameter.

Please cite this article in press as: Lim, H.K., Lee, J.-S., On the material properties of shell plate formed by line heating, International Journal of Naval Architecture and Ocean Engineering (2016), http://dx.doi.org/10.1016/j.ijnaoe.2016.08.001

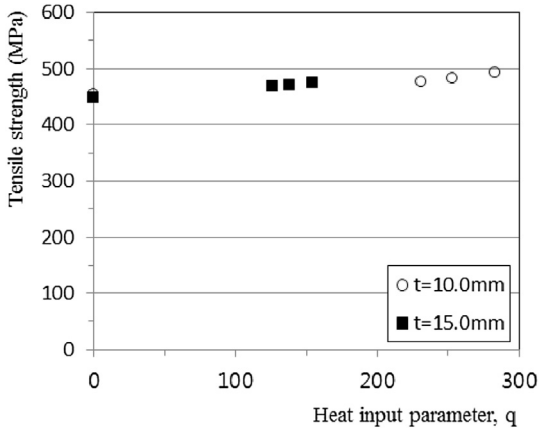


Fig. 16. Tensile strength vs heat input parameter.

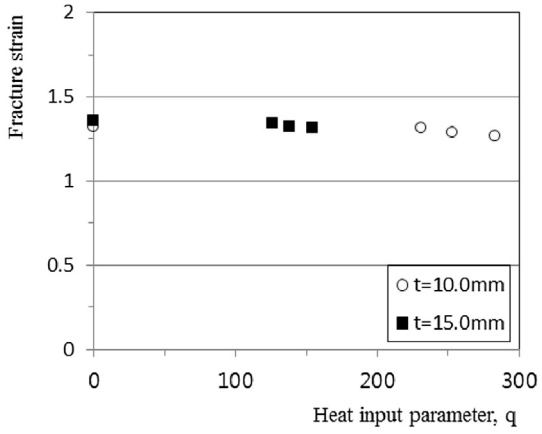


Fig. 17. Tensile strength vs heat input parameter.

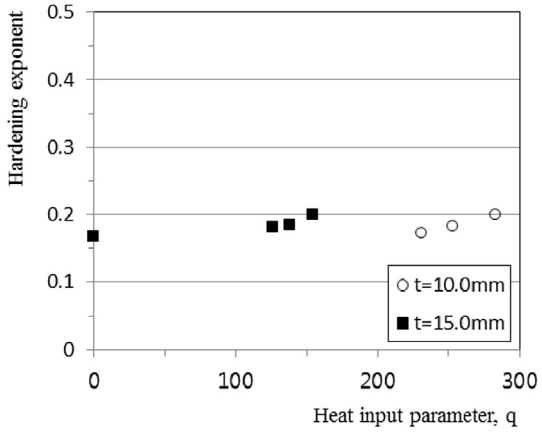


Fig. 18. Hardening exponent vs heat input parameter.

input parameter, $q$, much more case studies are needed in the further study.

## 4. Conclusions

This study is mainly concerned with investigating the effect of heat forming process on material properties of marine

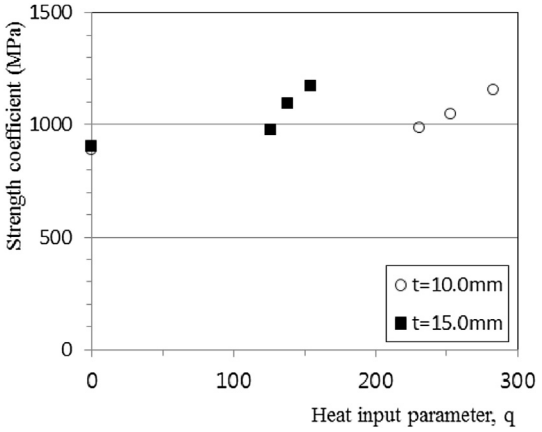


Fig. 19. Strength coefficient vs heat input parameter.

grade steel plate such as yield strength, tensile strength and so on with aiming at the rational structural design considering the accidental limit state such as collision. For the present study, line heating test has been carried out for 48 specimens of A-grade marine mild steel which is mainly used as shell plates found in bow and stern structure of a ship. Line heating test has been carried out with varying the affecting parameter such as heating speed and plate thickness. Based on the results of tension test for the heated specimens, change in several important mechanical properties has been proposed. From the results of the present tests, it is found that yield strength of heat formed steel plate has increased up to 25% and tensile strength by about 10% due to line heating. Meanwhile, elongation rate has decreased by about 5%.

Microscopic examination has been also conducted in order to observe the refined structures around the heated zone. From the present findings, it is seen that the grain refined zones like ferrite and pearlite are formed around the heat affected zone. Martensite transition is not, however, found in the present microscopic examination. This is due to the reason that ferrite phase exists as fine grains which are not able to transit into austenite phase and grow due to relatively low peak temperature when water cooling method is applied.

As it was described in this paper, this study is principally aimed at investigating plastic and rupture characteristics of shell plates heated by line heating method for a more rational design considering the accidental limit state. The data suggested in this study is expected to be used as fundamental materials to investigate the structural behaviour characteristics of ship. Based on the present experimental results, it is found that the five material properties, that is, yield strength, tensile strength, fracture strain, hardening exponent and strength coefficient vary with plate thickness and heat input. Hence the formulae relating the material properties and heat input parameter should be derived after performing more experimental and numerical works with varying affecting parameters within wider range. This will be presented in the judicial proceedings or journals in the near future.

Please cite this article in press as: Lim, H.K., Lee, J.-S., On the material properties of shell plate formed by line heating, International Journal of Naval Architecture and Ocean Engineering (2016), http://dx.doi.org/10.1016/j.ijnaoe.2016.08.001

## Acknowledgement

This paper is a part of research supported by University of Ulsan (Project No. : 2012-0182).

## References

Amdalh, J., 1983. Energy Absorption in Ship-platform Impacts. The University of Trondheim, Trondheim. Report No. UR-83–34.

ASTM E8, 2004. Standard Test Methods from Tensile Testing of Metallic Materials. American Society for Testing and Materials.

Bridgman, P.W., 1952. Studies in Large Plastic Flow and Fracture. McGraw-Hill, New York.

Choung, J.M., 2007. On the Fracture Criteria of Steels for Marine Structures Subjected to Impact Loadings. University of Ulsan. Ph.D Thesis.

Ha, Y.S., 2001. A Study on the Prediction of Plate Deformation by Heating of Weaving Path in Thick Plate Bending. Seoul National University. Master Thesis.

IACS, 2013. Common Structural Rules. Part 1, Chapter 5 Hull Girder Strength, Section 3 Hull Girder Residual Strength. International Association of Classification Societies.

Jang, C.D., Ko, D.E., Kim, B.I., Park, J.U., 2001. An experimental study of characteristics of plate deformation by heating process. J. Soc. Nav. Archit. Korea 38 (2), 62–70.

JIS Z 2201, 1998. Test Pieces for Tensile Test for Metallic Materials.

Kalpakjian, S., Schmid, S.R., 2001. Manufacturing Processes for Engineering Materials. KOEM (Korea Maritime Environment Management Corporation). www.kmprc.or.kr.

Lee, B.I., Yoo, H.S., Byun, G.G., Kim, H.G., 2002. A study on automation of steel plate forming by heating method. J. Soc. Nav. Archit. Korea 39 (2), 34–44.

Lee, J.S., 1996. Plate forming automation system of steel plates by line heating method (II). J. Soc. Nav. Archit. Korea 33 (3), 81–93.

Lee, J.S., 1997. Plate forming automation system of steel plates by line heating method (III). J. Soc. Nav. Archit. Korea 34 (2), 85–89.

Lehmann, E., Yu, X., 1998. On ductile rupture criteria for structural tear in case of ship collision and grounding. In: 7th International Symposium on Practical Design of Ships and Mobile Units, pp. 149–156.

Masubuchi, K., 1980. Analysis of Welded Structure. Pergamon Press, Oxford.

Minorsky, V.U., 1958. An analysis of ship collisions with reference to protection of nuclear power plants. J. Ship Res. 8.

Nomoto, T., Ohmori, T., Enosawa, M., Aoyama, K., Saitoh, M., 1990. Developement of simulator for plate bending by line heating. J. Soc. Nav. Archit. Jpn. 168, 527–535.

Satoh, K., Terasaki, T., 1976. Effect of welding conditions on welding deformations in welded structural materials. J. Jpn. Weld. Soc. 45 (4).

Shin, J.G., 1992. A two-dimensional simulator for plate forming by line heating. J. Soc. Nav. Archit. Korea 29 (1), 191–200.

Urban, J., 2003. Crushing and Fracture of Lightweight Structures. Technical University of Denmark.

Wisniewski, K., Koiakowski, P., 2003. The effect of selected parameters on ship collision results by dynamic FE simulation. Finite Elem. Anal. Des. 39, 985–1006.

Please cite this article in press as: Lim, H.K., Lee, J.-S., On the material properties of shell plate formed by line heating, International Journal of Naval Architecture and Ocean Engineering (2016), http://dx.doi.org/10.1016/j.ijnaoe.2016.08.001